HHS Public Access

Author manuscript

Cell. Author manuscript; available in PMC 2017 July 14.

Published in final edited form as:

Cell. 2016 July 14; 166(2): 358–368. doi:10.1016/j.cell.2016.05.025.

Enhancer control of transcriptional bursting

Takashi Fukaya[1,*], **Bomyi Lim**[1,*], and **Michael Levine**[1,2,†]

[1]Lewis-Sigler Institute for Integrative Genomics, Princeton University, Princeton, NJ 08544, USA

[2]Department of Molecular Biology, Princeton University, Princeton, NJ 08544, USA

Summary

Transcription is episodic, consisting of a series of discontinuous bursts. Using live imaging methods and quantitative analysis, we examine transcriptional bursting in living Drosophila embryos. Different developmental enhancers positioned downstream of synthetic reporter genes produce transcriptional bursts with similar amplitudes and duration, but generate very different bursting frequencies, with strong enhancers producing more bursts than weak enhancers. Insertion of an insulator reduces the number of bursts and the corresponding level of gene expression, suggesting that enhancer regulation of bursting frequency is a key parameter of gene control in development. We also show that linked reporter genes exhibit coordinated bursting profiles when regulated by a shared enhancer, challenging conventional models of enhancer-promoter looping.

Graphical abstract

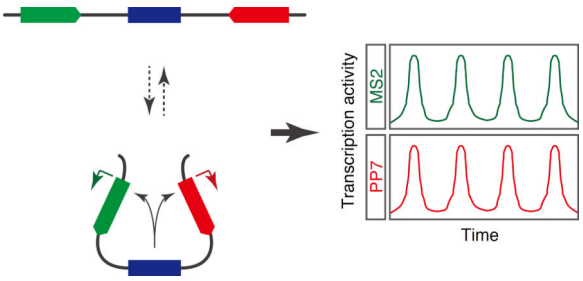

Shared enhancer drives coordinated transcriptional bursts

Introduction

Quantitative detection methods suggest that transcriptional bursting is a general property of gene expression in a variety of organisms, including bacteria, yeast, *Dictyostelium*,

†Correspondence should be addressed to M.L. msl2@princeton.edu.
*These authors contributed equally to this work

Author Contributions

T.F. performed the experiments and B.L. performed the image analysis. T.F., B.L. and M.L. designed the experiments, analyzed the results and wrote the manuscript.

Drosophila embryos, and cultured mammalian cells (Sanchez and Golding, 2013; Chong et al., 2014). These bursts are highly variable, but are thought to produce several transcripts per event. That is, consecutive RNA polymerase complexes are released from an active promoter during a period of several minutes, followed by a refractory period with little or no activity.

The first evidence for bursting was obtained over 35 years ago using electron microscopy on chromosome spreads from early *Drosophila* embryos (McKnight and Miller, 1979). Discrete chromosomal segments were found to contain sequential clusters of nascent RNAs separated by regions lacking detectable transcripts. More recent quantitative *in situ* hybridization assays and live-imaging methods provide additional support for discontinuities in transcription, or bursts (Coulon et al., 2013). For example, stochastic profiles of gene activity have been documented among the different cells of yeast populations (Lenstra et al., 2015). This variation is thought to arise, at least in part, from uncoordinated bursts of transcription. Visualization of living yeast, *Dictyostelium* and cultured mammalian cells provides further support for sporadic and uncoordinated bursts across cell populations (Yunger et al., 2010; Larson et al., 2011; Suter et al., 2011; Corrigan et al., 2016).

Here, we employ live-imaging methods to visualize transcriptional bursting during nuclear cycle (nc) 14, the one-hour interval of *Drosophila* development when the fate map of the adult fly is established by the localized expression of hundreds of zygotic patterning genes. Recent studies have examined the expression dynamics produced by two of the best-defined enhancers in the *Drosophila* embryo, the *hunchback* (*hb*) proximal enhancer and the *even-skipped* (*eve*) stripe 2 enhancer (Garcia et al., 2013; Lucas et al., 2013; Bothma et al., 2014). The *eve* stripe 2 enhancer directs a stripe of transcription at the future head/thorax boundary in response to combinatorial inputs, the Bicoid and Hunchback activators along with the Giant and Krüppel repressors (Small et al., 1992). Quantitative traces of individual nuclei revealed bursts of *eve* transcription during nc 14. These bursts are highly variable, but persist for an average of 5–7 minutes and are thought to produce tens of transcripts per burst (Bothma et al., 2014).

To explore the relationship between enhancers and bursts, we visualized and measured the activities of several well-defined enhancers in living *Drosophila* embryos. These enhancers were placed upstream or downstream of reporter genes containing a series of MS2 stem loops, permitting detection of nascent RNAs using MCP-GFP fusion proteins (Bertrand et al., 1998). We observed a correlation between enhancer strength and the frequency of transcriptional bursting. For example, the *snail* (*sna*) distal shadow enhancer generates more bursts than the proximal primary enhancer, although the amplitude and duration of the bursts are similar for the two enhancers. A variety of additional evidence, including insertion of the *gypsy* insulator (Cai and Levine, 1995), leads us to conclude that the regulation of bursting frequencies is a key parameter of gene control in the *Drosophila* embryo.

To determine the relationship between enhancer-promoter interactions and bursting frequencies, we simultaneously visualized two different reporter genes containing MS2 (Bertrand et al., 1998) or PP7 (Larson et al., 2011) stem loops under the control of individually linked enhancers. To our surprise, we observed a high frequency of coordinate bursts, suggesting co-activation of the two reporter genes. These observations challenge

classical models of stable enhancer-promoter looping and raise the possibility that chromosome topology is a critical feature of gene control in development.

Results

Bursting frequency and enhancer topology

We performed live-imaging of *MS2-yellow* reporter genes containing the full-length 1.5 kb *sna* shadow enhancer, a minimal 100 bp *sna* promoter (Lagha et al., 2013), and the complete *yellow* transcription unit (Figure 1A and B). The enhancer was initially placed 1 kb upstream of the promoter. The reporter gene was modified by insertion of a 1 kb sequence derived from *lacZ* into the intron of the *yellow* transcription unit (Figure 1B). This insertion does not alter normal splicing of *yellow* mRNAs (Figure S1A and B). The 5´ UTR of the reporter contains 24 copies of the MS2 RNA stem loop (Figure 1B), which permit detection of *yellow* nascent RNAs using a MCP-GFP fusion protein. Transgenes were integrated into specific genomic locations via phiC31-mediated transgenesis (Groth et al., 2004; Venken et al., 2006).

Fluorescent *in situ* hybridization indicates faithful expression of the *yellow* reporter gene in relation to the endogenous *sna* pattern (Figure S1C). Deletion of the *sna* shadow enhancer completely abolishes reporter gene expression (Figure S1C), indicating that neither the MS2 repeats nor *lacZ* sequence influences expression of the *yellow* reporter gene. Quantitative measurements also suggest that expression of *MS2-yellow* entirely relies on the presence of the enhancer (Figure S1D; Movie S1).

Transgenic males carrying the MS2 reporter gene were mated with virgin females that express MCP-GFP fusion proteins under the control of a maternal *nanos* promoter (see Experimental Procedures). Living embryos were examined using either a Zeiss 780 or Zeiss 880 confocal microscope. We monitored transcription during nc 14, which extends for ~50 min (at 25 °C) and culminates in the invagination of the mesoderm during the onset of gastrulation. *MS2-yellow* nascent RNAs were measured and an average of ~650 nuclei were examined for each transgene, including three biological replicates per experiment.

These measurements indicate erratic profiles of transcription during nc 14 (Figure 1C; Movie S2). It is possible that these discontinuities represent consecutive bursts that are too frequent to discern as individual events. That is, Pol II complexes released during a burst might not have time to clear the template before the onset of the subsequent burst (see Discussion). Some evidence for this possibility stems from the visualization of discrete bursts when the MS2 reporter gene is expressed in embryos containing reduced levels of the Dorsal activator (B. Lim, unpublished data).

Individual bursts were also observed when the 1.5 kb *sna* shadow enhancer was repositioned downstream of the *MS2-yellow* reporter gene, 7.5 kb from the transcription start site (Figure 1B; bottom). There is a reduction in the levels of expression as compared with transgenes containing the enhancer in the 5´ position (Figure 1E and Figure S1D and E). Nuclear traces exhibit discrete transcriptional bursts with an average duration of ~4 min (Figure 1D, compare with Figure 1C; also see Figure S1F and Movie S3). We therefore focused most of

the remaining analysis on transgenes containing distal 3′ enhancers. Moreover, this distance of 7.5 kb is similar to the median separation (~10 kb) between promoters and developmental enhancers based on whole-genome assays in *Drosophila* embryos (Kvon et al., 2014).

Differential bursting frequencies

The endogenous *sna* locus is regulated by both the distal shadow enhancer and a proximal primary enhancer located immediately upstream of the transcription start site (Ip et al., 1992b; Perry et al., 2010) (summarized in Figure 1A). The two enhancers possess overlapping regulatory activities in the presumptive mesoderm, but the proximal primary enhancer is weaker than the distal shadow enhancer (Dunipace et al., 2011; Bothma et al., 2015). To determine the basis for this difference, we placed the 2.8 kb primary enhancer downstream of the *MS2-yellow* reporter gene (Figure 2A). The transgene exhibits fewer bursts than the corresponding transgene containing the stronger shadow enhancer (Figure 2B; compare with Figure 2C). In contrast, there is a small but insignificant difference in the amplitudes of the bursts obtained with the two enhancers (Figure 2E). The major difference in the calculated total output of nascent RNAs produced by the *sna* primary and shadow enhancers can be attributed to bursting frequencies. The stronger shadow enhancer produces more bursts than the weaker primary enhancer.

To determine whether differential bursting frequencies underlie dynamic patterns of gene expression, we examined transgenes containing the *rhomboid* (*rho*) NEE, *Krüppel* (*Kr*) CD2 and *Abdominal-B* (*Abd-B*) IAB5 enhancers (Figure 2D) (Hoch et al., 1990; Ip et al., 1992a; Busturia and Bienz, 1993). Each of these enhancers mediates dynamic expression patterns that undergo spatial shifts or refinements during nc 14. As seen for the *sna* enhancers, there appears to be a close correspondence between the levels of expression and bursting frequencies (Figure 2E and Figure S2A–F and Figure S3). Moreover, the calculated total output of nascent RNAs produced per burst are quite similar among the different enhancers (Figure S2G), highlighting the importance of bursting frequencies in the control of gene activity. The only significant reduction in bursting amplitude is seen for the *Kr* CD2 enhancer (Figure 2E and Figure S2G). However, even in this case, reduced total output is mainly attributable to bursting frequency (~85%) rather than burst size (~15%), again supporting the general trend that bursting frequency is the most important parameter controlling gene activity.

We next compared the bursting frequencies within different regions of the *sna* and *Kr* expression patterns. *sna* exhibits similar levels of expression throughout the presumptive mesoderm (Kosman et al., 1991; Boettiger and Levine, 2013), whereas *Kr* exhibits differential levels of expression in the presumptive thorax with peak levels in central regions (Jaeger et al., 2004). The *sna* transgene exhibits similar bursting profiles across the presumptive mesoderm (Figure 3A–C and Figure S4A). In contrast, the *Kr* CD2 transgene exhibits differential bursting profiles, whereby nuclei present in central regions exhibit over twice as many bursts as those located in posterior regions (Figure 3D–F and Figure S4A). The analysis of the *rho* NEE and IAB5 enhancers lends further support for the proposal that differential spatial and temporal patterns of gene expression depend on varying bursting frequencies (Figure S4B–D).

We next asked whether bursting dynamics are affected by the core promoter. The *sna* promoter contained in the *MS2-yellow* transgenes was replaced by either a minimal *eve* or minimal *sog* promoter sequence (Figure S5A). qRT-PCR assays suggest that the *eve* and *sna* promoters possess similar activities, while the *sog* promoter is significantly weaker (Figure S5B). Indeed, the *eve* and *sna* promoters exhibit similar bursting frequencies and amplitudes (Figure S5C and E), whereas the *sog* promoter causes reductions in both bursting frequencies and amplitude (Figure S5D and E). It therefore appears that the *sog* promoter makes inefficient contact with distal enhancers, and releases a small number of Pol II complexes upon activation. It is possible that this inefficient activation is due to the absence of a promoter-proximal tethering element, as seen for *brinker*, which exhibits a similar profile of expression (Dunipace et al., 2013).

Promoter competition and co-activation

When multiple genes are under the control of a shared enhancer, proximal promoters tend to sequester the enhancer and thereby diminish activation of distal promoters (Choi and Engel, 1988; Foley and Engel, 1992). To determine whether this type of promoter competition influences bursting frequencies, we created transgenes containing two separate reporter genes, *MS2-yellow* and *PP7-yellow*, which contains 24 copies of the PP7 RNA stem loop sequence (Larson et al., 2011). The *PP7-yellow* reporter gene was placed in two different orientations, symmetric and asymmetric (Figure 4A). In the symmetric orientation, the shared 3′ *sna* shadow enhancer is equidistant (~7.5 kb) from the MS2 and PP7 reporter genes (Figure 4A; top). In the asymmetric configuration, the enhancer maps much closer (~1 kb) to *PP7-yellow* than *MS2-yellow* (Figure 4A; bottom).

The transcriptional activities of the two reporter genes were visualized in living embryos using MCP-GFP and tdTomato-PCP fusion proteins. In the symmetric configuration, the reporter genes exhibit similar bursting frequencies during nc 14 (Figure 4B and C). In contrast, when inverted, the proximal *PP7-yellow* reporter gene displays sustained transcription as seen when the *sna* shadow enhancer is placed 1 kb upstream of the MS2 reporter gene (Figure 4D; compare with Figure 1C). This augmented expression of the proximal *PP7-yellow* reporter gene is accompanied by less frequent bursting of the distal *MS2-yellow* gene (Figure 4E; compare with Figure 4C). It therefore appears that promoter competition diminishes the expression of the distal promoter by reducing the frequency of transcriptional bursts (Figure 4F). Moreover, these studies indicate that linked MS2 and PP7 reporter genes can produce different bursting profiles in the same embryo.

We next applied two-color MS2/PP7 live imaging to explore the dynamics of gene activation by a shared enhancer. Classical studies using fixed embryos suggest activation of linked reporter genes during the ~1 hr interval of nc 14 (Gray et al., 1994; Cai and Levine, 1997; Ohtsuki and Levine, 1998). Recent 4C-Seq assays also provide evidence for activation of linked genes by a shared enhancer within the native genome (Ghavi-Helm et al., 2014), although the dynamics of these interactions are uncertain.

According to classical looping models, we would expect the shared enhancer to randomly select one of the linked promoters, linger for a few minutes to produce a burst, dissociate, and then repeat the process. According to this scenario, we would observe sequentially

alternating expression of the MS2 (green) and PP7 (red) reporter genes. We created a series of reporter genes containing different developmental enhancers (*sna* shadow, *sna* primary, *rho* NEE, *Kr* CD2 or IAB5) positioned between symmetric, convergent *MS2-yellow* and *PP7-yellow* reporter genes (Figure 5A). To our surprise, most nuclei exhibit coordinated transcriptional bursts of both reporter genes (Figure 5B–E; Movie S4). In a typical nucleus, approximately two-thirds of the bursts are coordinated while the others are offset (Figure 5C; Movie S5). We define coordinate bursts as those exhibiting at least 70% overlap in onset and duration (see Experimental Procedures).

Because the strong *sna* shadow enhancer produces so many bursts, it is hard to tell whether coordinate bursts are produced by chance. We therefore used weaker enhancers, such as the *sna* primary enhancer and the *Kr* CD2 enhancer, which produce fewer bursts. The temporal resolution reveals significant coordination of PP7 and MS2 bursting (Figure 5D–G and Figure S6A and B; Movie S6). In the specific nuclei that are shown, over half the bursts from each transgene exhibit coordinate, or nearly coordinate, dynamics (Figure 5D and E and Figure S6A and B). Similar coordination was observed when the minimal *sna* promoter was replaced with either the *eve* or *sog* promoters (Figure S7). To determine whether coincident bursts could occur by chance, we performed computational simulations that assume independent activation of the PP7 and MS2 reporter genes by pairing random trajectories of PP7 and MS2 with similar bursting frequencies. Such simulations predict just ~25% correspondence in the bursts, which is significantly lower than the observed frequencies of coordinate bursting (Figure 5F and G; right).

A potential complication in our analysis is the precocious replication of most genetic loci during the onset of nc 14 (Foe and Alberts, 1983; Edgar and O'Farrell, 1990). It is possible that an enhancer on each chromatid (or amplicon) generates bursts of MS2 and PP7 reporter genes independently, giving the appearance of co-activation. However, the observation that both strong (e.g., *sna* shadow) and weak (e.g., *rho* NEE) enhancers exhibit frequent (60–70%) coordination of MS2/PP7 bursts is inconsistent with this explanation. Computer simulations that assume independent regulation of the two sister chromatids reveal significantly fewer (~20%) coordinate bursts (Figure S6C).

Enhancer dynamics altered by the *gypsy* insulator

Coordinate bursting of two reporter genes by a shared enhancer raises the possibility of a higher order chromosomal topology that positions the enhancer near both promoters (see Discussion). We explored this possibility by inserting the *gypsy* insulator DNA between the *sna* shadow enhancer and *PP7-yellow* reporter gene (Figure 6A). As expected, the insulator greatly diminishes the levels of *PP7-yellow* expression without significantly altering expression of the *MS2-yellow* reporter gene (Figure 6B–E). This is consistent with previous studies suggesting that insulator DNAs selectively block interactions of distal enhancers with their target promoters (Cai and Levine, 1995). However, the *gypsy* insulator does not completely eliminate expression of the *PP7-yellow* reporter gene, but results in a several-fold reduction (Figure 6E). Comparison of the PP7 reporter genes with or without the insulator suggests a correspondence between the levels of expression and the frequency of bursts (Figure 6E).

To our surprise, the infrequent PP7 bursts tend to coincide with MS2 bursts (Figure 6C and D). The separation of the MS2 and PP7 reporter genes into separate chromosomal loop domains would be expected to uncouple their coordinated bursting behaviors. Instead, ~75% of all PP7 bursts coincide with MS2 bursts (Figure 6F). This observation raises the possibility that neighboring chromosomal loop domains may be dynamic and adopt alternative configurations (Figure 7; see Discussion).

Discussion

We have presented several lines of evidence that the regulation of bursting frequencies is a key parameter of gene control in the *Drosophila* embryo. Strong enhancers produce more bursts than weak enhancers. Moreover, differential bursting frequencies correlate with nonuniform expression profiles of *rho*, *Abd-B*, and *Kr*. To determine the relationship between enhancer-promoter interactions and bursts, we examined the regulation of linked MS2 and PP7 reporter genes by shared enhancers. To our surprise we observed a high incidence of coordinate bursts, suggesting co-activation of linked reporter genes. These observations challenge traditional models of enhancer-promoter looping, as discussed below.

Regulation of bursting frequencies

Previous live imaging studies revealed bursts of *eve* stripe 2 expression, but not *hb* (Garcia et al., 2013; Lucas et al., 2013; Bothma et al., 2014). We propose that the high levels of gene activity mediated by the proximal *hb* enhancer obscure individual bursts (Garcia et al., 2013; Lucas et al., 2013). Given the rates of Pol II elongation (~2.0 kb / min) (Ardehali and Lis, 2009), it should take about three minutes for all of the Pol II complexes from a burst to clear the reporter gene template. Consequently, refractory periods lasting less than three minutes would be expected to result in the conflation of consecutive bursts. It appears that we circumvented this problem by placing test enhancers downstream of the reporter gene, thereby diminishing the levels of expression and permitting the resolution of discrete bursts (Figure 1D).

In principle, the levels of gene activity can be regulated by modulating the duration, amplitude, or frequency of individual bursts. We consistently observe that bursting frequency is the major parameter underlying differences in gene expression. Most notably, the insertion of the *gypsy* insulator DNA between the *sna* shadow enhancer and PP7 reporter gene results in a marked reduction in the levels of gene expression and a corresponding diminishment in the number of bursts (Figure 6). However, when bursts are detected, they exhibit nearly the same amplitude as those seen for the unimpeded enhancer lacking the insulator DNA. There are minor reductions in the amplitude (e.g., rate of release of Pol II complexes from the promoter) and duration (how long the promoter remains active), but bursting frequency is the most consistent variable we have observed (Figure 6E).

We propose that transcriptional bursting renders gene expression more immediately responsive to dynamic and transient on and off signals during development. For example, the *eve* stripe 2 enhancer is regulated by localized repressors that delineate the anterior and posterior stripe borders (Small et al., 1992). This repression tends to occur during the refractory period between bursts (Bothma et al., 2014). Perhaps it is easier to repress

transcription during these “down” phases as compared with periods of peak activity. Bursting may be an essential property of gene activity, and it is easy to imagine that the regulation of bursting frequencies is a prime determinant of gene control in a variety of developmental processes.

Enhancer-promoter communication

According to conventional looping models (e.g., Su et al., 1991), we expected the shared enhancer to randomly select one of the two promoters, generate a burst, dissociate from the target promoter and again randomly select a reporter gene for another burst. This would lead to alternating red (*PP7-yellow*) and green (*MS2-yellow*) bursts. Instead, we see a high incidence of coordinate bursting (Figure 5), raising the possibility that an enhancer can simultaneously activate linked promoters separated by a distance of over 15 kb. Co-activation is seen even when an insulator DNA is inserted between the shared enhancer and one of the reporter genes (Figure 6). These observations suggest a far more dynamic view of enhancer-promoter interactions than the stable landscapes implied by 4C assays (e.g., Ghavi-Helm et al., 2014).

Most enhancer-promoter interactions are thought to occur in the context of topological association domains (TADs) (reviewed by Gibcus and Dekker, 2013). In vertebrates, a typical TAD is ~1 Mb in length and contains 10 genes and a few hundred enhancers. TADs are thought to be static structures that are invariant in different tissues. Despite this invariance, enhancer-promoter interactions within TADs appear to be highly dynamic. The co-activation of linked MS2 and PP7 reporter genes might result from local loop domains that bring different target promoters into close proximity with shared enhancers (Figure 7A). The alternating inhibition and coordinate bursting observed for transgenes containing the *gypsy* insulator (Figure 7B) is consistent with the occurrence of dynamic transitions in loop domains. Such transitions might also be due to unstable assembly of insulator protein complexes, which consist of multiple subunits including Su(Hw), Mod(mdg4)2.2 and CP190 (Ghosh et al., 2001; Pai et al., 2004; Schoborg et al., 2013). Just as live-imaging methods provide a far more dynamic view of gene activity in the *Drosophila* embryo as compared with fixed tissues (e.g., Bothma et al., 2014), these methods are likely to provide a more vibrant glimpse into the nature of enhancer-promoter communication.

Experimental procedures

Site specific transgenesis by phiC31 system

All reporter plasmids were integrated into a unique landing site on chromosome 3 using strain 9750 (Bloomington *Drosophila* Stock Center). The *nanos>SV40NLS-tdTomato-PCP* expression plasmid was integrated into a unique landing site on chromosome 2 using strain 9723 (Bloomington *Drosophila* Stock Center). Microinjection was performed as described (Fish et al., 2007).

Fly strains

Maternal expression of the MCP-GFP fusion protein was obtained using a transgenic strain carrying a *nanos>MCP-GFP* transgene that was integrated onto the third chromosome by P-

element mediated transformation (Garcia et al., 2013). Maternal expression of the tdTomato-PCP fusion protein was obtained using a transgenic strain carrying a *nanos>SV40NLS-tdTomato-PCP* transgene on the second chromosome. These were mated to create the fly line *yw*; *nanos>SV40NLS-tdTomato-PCP*; *nanos>MCPGFP* in order to obtain co-expression of both MCP-GFP and tdTomato-PCP. The fly line *yw*; *His2Av-mRFP*; *nanos>MCP-GFP* was previously described (Garcia et al., 2013)

In situ hybridization

Embryos were dechorionated and fixed in 0.5× PBS, 25 mM EGTA, 4% formaldehyde and 50% Heptane for 20 min. Antisense RNA probes labeled with digoxigenin or biotin were used to detect RNAs. Detection was carried out with anti-digoxigenin and antibiotin primary antibodies (Roche) and fluorescent secondary antibodies (Molecular Probes). Imaging was performed on a Zeiss LSM 780 confocal microscope.

Quantitative RT-PCR

Total RNA was extracted from fifteen embryos at nuclear cycle 14 using TRIzol reagent (Thermo Fisher Scientific) and cDNA was synthesized with QuantiTect Reverse Transcription Kit (Qiagen). Quantitative PCR was performed using SYBR Green PCR Master Mix (Thermo Fisher Scientific). Each experiment was performed in biological triplicates with technical duplicates. Relative RNA levels were calculated by the 2-ΔΔC(t) method and normalized to *rp49* levels. Primers (5′-GCG TAC ATC GGG CAA ATA ATA TC-3′) and (5′-TAA TCA CGA CGC GCT GTA TC-3′) were used for *MS2-yellow* and primers (5′-GCA CCA AGC ACT TCA TCC-3′) and (5′-AGC GGC GAC GCA CTC TGT-3′) were used for *rp49*.

Live imaging

yw; *His2Av-mRFP*; *nanos>MCP-GFP* or *yw*; *nanos>SV40NLS-tdTomato-PCP*; *nanos>MCP-GFP* virgins were mated with males carrying the MS2 and PP7 reporter genes. The resulting embryos were dechorinated and mounted between a semipermeable membrane (In Vitro Systems & Services) and a coverslip (25 mm × 25 mm) and embedded in Halocarbon oil 27 (Sigma). Embryos were imaged using a Zeiss LSM 780 (Figure 4–6) and Zeiss LSM 880 confocal microscope (Figure 1–3). Plan-Apochromat 40× / 1.4N.A. oil immersion objective was used for Zeiss LSM 780 and Plan-Apochromat 40× / 1.3N.A. oil immersion objective was used for Zeiss LSM 880. The pixel size was set to 490 nm and a single image consisted of 512 × 512 pixels. At each time point, a stack of 21 images separated by 0.5 μm was acquired and the final time resolution is 20 sec. Images were captured in 16 bit. For each reporter line, three biological replicates were taken using the same setting of the microscope. The same laser power and microscope setting were used for the datasets shown in Figure 1–3, and another setting was used for the datasets shown in Figure 4–6. The latter datasets focus on the analysis of coordinate bursting of the linked *MS2-yellow* and *PP7-yellow* reporter genes. For this purpose it was necessary to reduce the laser power in order to minimize the photobleaching of the tdTomato-PCP fusion protein.

Image Processing

For each time point, maximum projections were obtained for all 21 z-sections per image. General image processing steps are as follows; I) nuclei segmentation, II) nuclei tracking, and III) *MS2-yellow* and *PP7-yellow* signal recording. All image processing and analysis scripts were implemented in MATLAB (R2015a, MathWorks).

Nuclei segmentation

For movies analyzed in Figures 1–3, His2Av-mRFP was used to label nuclei. For movies analyzed in Figures 4–6, tdTomato-PCP contains the NLS, which permits visualization of nuclei. For these latter movies, nuclei become visible ~10 minutes after the onset of nc 14, whereas the analysis of movies used for Figures 1–3 spans the entirety of nc 14. Nuclei-labeled channels (His2Av-mRFP or tdTomato-PCP) were first blurred with the Gaussian filter to generate smooth images. Then top-hat filtering and contrast-limited adaptive histogram equalization were used to remove any potential uneven illumination on the images and to enhance contrast (Zuiderveld, 1994). Processed images were converted into binary images, using a threshold value obtained using Otsu's method (Otsu, 1975). Binary images from each frame were manually checked to ensure correct segmentation. The processed images were used only to segment the nuclei, whereas raw image files were subsequently used to record *MS2-yellow* and *PP7-yellow* signals. From each segmented frame, the number of connected components (i.e. the number of nuclei that are segmented) was obtained and each component was indexed. For each indexed nucleus, x and y coordinates of all the pixels that constitute the nucleus as well as the coordinates of the center of mass of each nucleus were measured. During indexing, nuclei that are located at the edge of the frame were excluded from the analysis.

Nuclei tracking

A custom Matlab script was implemented to track individual nuclei during nc 14. Nuclei do not divide nor move drastically within the cycle until the onset of gastrulation. For each indexed nucleus in a given frame, the euclidean distances between that nucleus and all other nuclei in the next frame is determined. The nucleus with the minimum euclidean distance is chosen, and if that distance is smaller than 10 pixels, the pair of nuclei is grouped as a single entity. That is, if the distance between nucleus X from frame 1 and nucleus Y from frame 2 is the shortest, and less than 10 pixels, then they are considered to be the same. If the distance is bigger than 10 pixels, it is concluded that the nucleus does not have a corresponding lineage in the next frame. This often occurs when the nucleus is located near the edge and leaves the frame. In a typical movie, 250–300 unambiguous lineages were obtained for the duration of the analysis.

Recording MS2 and PP7 signals

Maximum projections of raw 16 bit TIFF images were used for recording signals. The fluorescent intensity of the brightest pixel within each nucleus was determined after subtracting the background nuclear signal. Since some of the transcription foci are located at the edge of the nucleus, our search area was 10% bigger than the area of each segmented nucleus. Since the size of transcription focus is bigger than a single pixel in our image

resolution, it was checked whether the brightest pixel within the nucleus is surrounded by other bright pixels. If not, intensity from the second or the third brightest pixel that is surrounded by other bright pixels was extracted. Through these steps, it was possible to remove some false-positives. In general, the signal-to-noise ratio of our live imaging movies was high enough to distinguish the real MS2/PP7 signals from the background noise. This process was repeated for all nuclei in each frame. Using the lineage information from the previous step, transcription activity of the *MS2-yellow* and *PP7-yellow* can be plotted for a single nucleus over time.

Description of bursting properties

From each trajectory, the number of bursts, the amplitude of each burst, and the total integrated signal (total nascent RNA) produced by each nucleus during nc 14 were measured. A burst is defined as a change in signal intensity whose dynamic range from peak to trough is at least twice the dynamic range from the baseline of the trajectory to the trough.

The peak of each burst was measured after smoothing the trajectories using the LOESS method (Cleveland, 1979). The amplitude was determined by taking the average of all the bursts in a single nucleus. The duration was determined by measuring the timespan of each burst above background, or above a trough (when the trough level is higher than the background). Total transcript production of a given nucleus during nc 14 was quantified by taking the area under the trajectory. Similarly, output per burst was determined by taking the area of a single burst.

Analysis of coordinate burst

The frequency of coordinate bursts from linked *MS2-yellow* and *PP7-yellow* reporter genes was obtained by quantifying how many MS2 bursts overlap PP7 bursts, or vice versa. Two bursts were defined as “coordinate” if the burst durations exhibited at least 70 % overlap.

Simulation of coordinate bursts among randomly selected nuclei

For all the trajectories in a given embryo, one trajectory for MS2 and another trajectory for PP7 with comparable number of bursts were randomly selected. Then the number of coordinate bursts from these trajectories was determined using the criteria described above.

Simulation of independent sister chromatid behavior

The following conditions were used to simulate transcriptional bursting of sister chromatids. Each chromatid can generate up to 6 bursts during the 50 min time window of analysis, and each burst lasts for 4 min. Each burst is assigned to either MS2 or PP7 with equal probability. The transcription activities from each chromatid were re-plotted as MS2 and PP7 trajectories over time. The frequencies of coordinate bursts from the MS2 and PP7 trajectories were calculated based on cut-off of 70% overlap in the onset and duration of each burst.

Supplementary Material

Refer to Web version on PubMed Central for supplementary material.

Acknowledgments

We thank Thomas Gregor for sharing the His2Av-mRFP; MCP-GFP fly strain. We also thank Samuel Pak Ng for assistance with fly injections, Evangelos Gatzogiannis for instruction and help with confocal imaging, and the Bloomington *Drosophila* Stock Center for fly strains. We are also grateful for members of the Levine laboratory for discussions. T.F was the recipient of a JSPS Research Fellowship for Research Abroad and is currently supported by a Human Frontier Science Program Long-Term Fellowship. This study was funded by grants from the National Institutes of Health (GM34431 and GM46638).

References

Ardehali MB, Lis JT. Tracking rates of transcription and splicing in *vivo*. Nat Struct Mol Biol. 2009; 16:1123–1124. [PubMed: 19888309]

Bertrand E, Chartrand P, Schaefer M, Shenoy SM, Singer RH, Long RM. Localization of *ASH1* mRNA particles in living yeast. Mol Cell. 1998; 2:437–445. [PubMed: 9809065]

Boettiger AN, Levine M. Rapid transcription fosters coordinate *snail* expression in the *Drosophila* embryo. Cell reports. 2013; 3:8–15. [PubMed: 23352665]

Bothma JP, Garcia HG, Esposito E, Schlissel G, Gregor T, Levine M. Dynamic regulation of eve stripe 2 expression reveals transcriptional bursts in living *Drosophila* embryos. Proc Natl Acad Sci U S A. 2014; 111:10598–10603. [PubMed: 24994903]

Bothma JP, Garcia HG, Ng S, Perry MW, Gregor T, Levine M. Enhancer additivity and non-additivity are determined by enhancer strength in the *Drosophila* embryo. Elife. 2015; 4

Busturia A, Bienz M. Silencers in *Abdominal-B*, a homeotic *Drosophila* gene. EMBO J. 1993; 12:1415–1425. [PubMed: 8096812]

Cai H, Levine M. Modulation of enhancer-promoter interactions by insulators in the *Drosophila* embryo. Nature. 1995; 376:533–536. [PubMed: 7637789]

Cai HN, Levine M. The *gypsy* insulator can function as a promoter-specific silencer in the *Drosophila* embryo. EMBO J. 1997; 16:1732–1741. [PubMed: 9130717]

Choi OR, Engel JD. Developmental regulation of β-*globin* gene switching. Cell. 1988; 55:17–26. [PubMed: 3167976]

Chong S, Chen C, Ge H, Xie XS. Mechanism of transcriptional bursting in bacteria. Cell. 2014; 158:314–326. [PubMed: 25036631]

Cleveland WS. Robust locally weighted regression and smoothing scatterplots. Journal of the American Statistical Association. 1979; 74:829–836.

Corrigan AM, Tunnacliffe E, Cannon D, Chubb JR. A continuum model of transcriptional bursting. eLife. 2016

Coulon A, Chow CC, Singer RH, Larson DR. Eukaryotic transcriptional dynamics: from single molecules to cell populations. Nat Rev Genet. 2013; 14:572–584. [PubMed: 23835438]

Dunipace L, Ozdemir A, Stathopoulos A. Complex interactions between cis-regulatory modules in native conformation are critical for *Drosophila snail* expression. Development. 2011; 138:4075–4084. [PubMed: 21813571]

Dunipace L, Saunders A, Ashe HL, Stathopoulos A. Autoregulatory feedback controls sequential action of cis-regulatory modules at the *brinker* locus. Developmental cell. 2013; 26:536–543. [PubMed: 24044892]

Edgar BA, O'Farrell PH. The three postblastoderm cell cycles of *Drosophila* embryogenesis are regulated in G2 by string. Cell. 1990; 62:469–480. [PubMed: 2199063]

Fish MP, Groth AC, Calos MP, Nusse R. Creating transgenic *Drosophila* by microinjecting the site-specific phiC31 integrase mRNA and a transgene-containing donor plasmid. Nat Protoc. 2007; 2:2325–2331. [PubMed: 17947973]

Foe VICTORIAE, Alberts BM. Studies of nuclear and cytoplasmic behaviour during the five mitotic cycles that precede gastrulation in I embryogenesis. Journal of cell science. 1983; 61:31–70. [PubMed: 6411748]

Foley KP, Engel JD. Individual stage selector element mutations lead to reciprocal changes in β-vs. ε-*globin* gene transcription: genetic confirmation of promoter competition during globin gene switching. Genes Dev. 1992; 6:730–744. [PubMed: 1577269]

Garcia HG, Tikhonov M, Lin A, Gregor T. Quantitative imaging of transcription in living *Drosophila* embryos links polymerase activity to patterning. Curr Biol. 2013; 23:2140–2145. [PubMed: 24139738]

Ghavi-Helm Y, Klein FA, Pakozdi T, Ciglar L, Noordermeer D, Huber W, Furlong EE. Enhancer loops appear stable during development and are associated with paused polymerase. Nature. 2014; 512:96–100. [PubMed: 25043061]

Ghosh D, Gerasimova TI, Corces VG. Interactions between the Su (Hw) and Mod (mdg4) proteins required for *gypsy* insulator function. The EMBO journal. 2001; 20:2518–2527. [PubMed: 11350941]

Gibcus JH, Dekker J. The hierarchy of the 3D genome. Molecular cell. 2013; 49:773–782. [PubMed: 23473598]

Gray S, Szymanski P, Levine M. Short-range repression permits multiple enhancers to function autonomously within a complex promoter. Genes Dev. 1994; 8:1829–1838. [PubMed: 7958860]

Groth AC, Fish M, Nusse R, Calos MP. Construction of transgenic *Drosophila* by using the site-specific integrase from phage phiC31. Genetics. 2004; 166:1775–1782. [PubMed: 15126397]

Hoch M, Schroder C, Seifert E, Jackle H. cis-acting control elements for *Krüppel* expression in the *Drosophila* embryo. EMBO J. 1990; 9:2587–2595. [PubMed: 2114978]

Ip YT, Park RE, Kosman D, Bier E, Levine M. The *dorsal* gradient morphogen regulates stripes of *rhomboid* expression in the presumptive neuroectoderm of the *Drosophila* embryo. Genes Dev. 1992a; 6:1728–1739. [PubMed: 1325394]

Ip YT, Park RE, Kosman D, Yazdanbakhsh K, Levine M. *dorsal-twist* interactions establish *snail* expression in the presumptive mesoderm of the *Drosophila* embryo. Genes Dev. 1992b; 6:1518–1530. [PubMed: 1644293]

Jaeger J, Surkova S, Blagov M, Janssens H, Kosman D, Kozlov KN, Manu, Myasnikova E, Vanario-Alonso CE, Samsonova M, Sharp DH, Reinitz J. Dynamic control of positional information in the early *Drosophila* embryo. Nature. 2004; 430:368–371. [PubMed: 15254541]

Kosman D, Ip YT, Levine M, Arora K. Establishment of the mesoderm-neuroectoderm boundary in the *Drosophila* embryo. Science. 1991; 254:118–122. [PubMed: 1925551]

Kvon EZ, Kazmar T, Stampfel G, Yáñez-Cuna JO, Pagani M, Schernhuber K, Dickson BJ, Stark A. Genome-scale functional characterization of *Drosophila* developmental enhancers *in vivo*. Nature. 2014

Lagha M, Bothma JP, Esposito E, Ng S, Stefanik L, Tsui C, Johnston J, Chen K, Gilmour DS, Zeitlinger J, Levine MS. Paused Pol II coordinates tissue morphogenesis in the *Drosophila* embryo. Cell. 2013; 153:976–987. [PubMed: 23706736]

Larson DR, Zenklusen D, Wu B, Chao JA, Singer RH. Real-time observation of transcription initiation and elongation on an endogenous yeast gene. Science. 2011; 332:475–478. [PubMed: 21512033]

Lenstra TL, Coulon A, Chow CC, Larson DR. Single-Molecule Imaging Reveals a Switch between Spurious and Functional ncRNA Transcription. Mol Cell. 2015; 60:597–610. [PubMed: 26549684]

Lucas T, Ferraro T, Roelens B, De Las Heras Chanes J, Walczak AM, Coppey M, Dostatni N. Live imaging of Bicoid-dependent transcription in *Drosophila* embryos. Curr Biol. 2013; 23:2135–2139. [PubMed: 24139736]

McKnight SL, Miller OLJ. Post-replicative nonribosomal transcription units in *D. melanogaster* embryos. Cell. 1979; 17:551–563. [PubMed: 113103]

Ohtsuki S, Levine M. GAGA mediates the enhancer blocking activity of the eve promoter in the *Drosophila* embryo. Genes Dev. 1998; 12:3325–3330. [PubMed: 9808619]

Otsu N. A threshold selection method from gray-level histograms. Automatica. 1975; 11:23–27.

Pai C-Y, Lei EP, Ghosh D, Corces VG. The centrosomal protein CP190 is a component of the *gypsy* chromatin insulator. Molecular cell. 2004; 16:737–748. [PubMed: 15574329]

Perry MW, Boettiger AN, Bothma JP, Levine M. Shadow enhancers foster robustness of *Drosophila* gastrulation. Curr Biol. 2010; 20:1562–1567. [PubMed: 20797865]

Sanchez A, Golding I. Genetic determinants and cellular constraints in noisy gene expression. Science. 2013; 342:1188–1193. [PubMed: 24311680]

Schoborg T, Rickels R, Barrios J, Labrador M. Chromatin insulator bodies are nuclear structures that form in response to osmotic stress and cell death. The Journal of cell biology. 2013; 202:261–276. [PubMed: 23878275]

Small S, Blair A, Levine M. Regulation of *even-skipped stripe 2* in the *Drosophila* embryo. EMBO J. 1992; 11:4047–4057. [PubMed: 1327756]

Su W, Jackson S, Tjian R, Echols H. DNA looping between sites for transcriptional activation: self-association of DNA-bound Sp1. Genes & Development. 1991; 5:820–826. [PubMed: 1851121]

Suter DM, Molina N, Gatfield D, Schneider K, Schibler U, Naef F. Mammalian genes are transcribed with widely different bursting kinetics. Science. 2011; 332:472–474. [PubMed: 21415320]

Venken KJ, He Y, Hoskins RA, Bellen HJ. P[acman]: a BAC transgenic platform for targeted insertion of large DNA fragments in *D. melanogaster*. Science. 2006; 314:1747–1751. [PubMed: 17138868]

Yunger S, Rosenfeld L, Garini Y, Shav-Tal Y. Single-allele analysis of transcription kinetics in living mammalian cells. Nature methods. 2010; 7:631–633. [PubMed: 20639867]

Zuiderveld K. Contrast limited adaptive histogram equalization. Graphics gems IV. 1994:474–485.

Highlights

- Transcriptional bursts are an important feature of gene activity in living embryos.
- The levels of gene activity depend on the frequency of transcriptional bursts.
- A single enhancer can co-activate two linked reporter genes.
- An insulator diminishes the frequency of bursts but not co-activation of linked genes.

In Brief

Fukaya and Lim *et al*. present an analysis of enhancer-promoter communication in living *Drosophila* embryos. They employ a combination of live imaging methods and quantitative analysis to measure gene activity in real time. These studies provide evidence that enhancers regulate the frequency of transcriptional bursts. Strong enhancers produce more bursts than weak enhancers. Shared enhancers are able to coactivate linked reporter genes, suggesting the importance of chromosome topology in gene control.

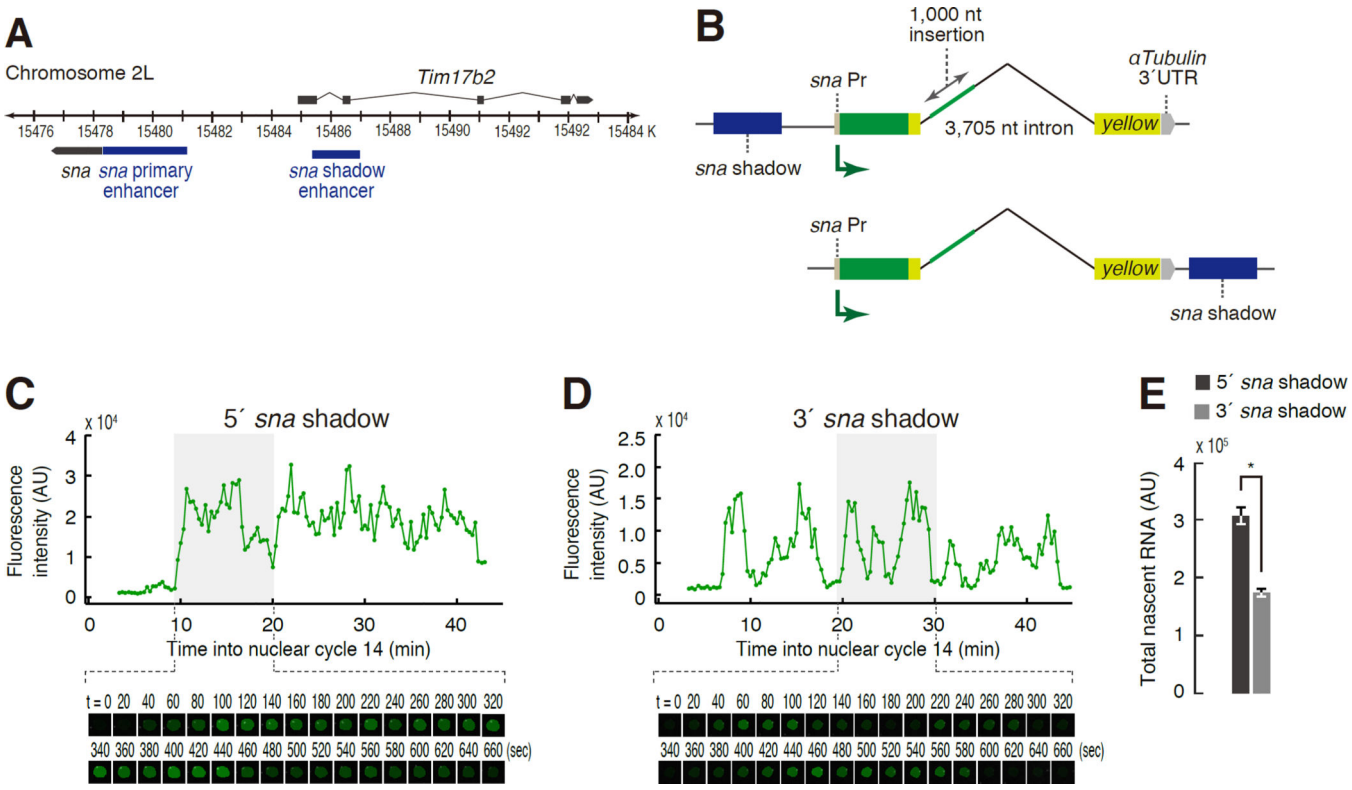

Figure 1. Enhancer location influences transcriptional dynamics

(A) The *sna* locus contains the proximal primary enhancer adjacent to the promoter, as well as a distal shadow enhancer located in the neighboring *Tim17b2* locus.

(B) Schematic representation of *yellow* reporter gene containing the 100 bp minimal *sna* promoter and 24× MS2 RNA stem loops within the 5′ UTR. 1.5 kb *sna* shadow enhancer was placed either 1 kb upstream (5′ *sna* shadow enhancer; top) or 7.5 kb downstream (3′ *sna* shadow enhancer; bottom) of the promoter. This reporter gene also contains a linked *snaPr-PP7-yellow* in symmetric location that will be discussed in Figures 4 and 5.

(C, D) Representative traces of transcription activity in individual nuclei. Snapshots are taken from the nucleus that was used to measure the corresponding traces. The intensity of green false-color is proportional to the signal strength of the transcription focus at a given time.

(E) Average values of total transcripts produced per nucleus. The output was measured by quantifying the area under the curve for individual traces. A total of 614 and 907 nuclei, respectively, were measured from three individual embryos for the reporter genes with 5′ and 3′ *sna* shadow enhancer. The error bars represent the standard deviation of the mean of three biological replicates. Asterisk indicates $p < 0.01$. See also Figure S1.

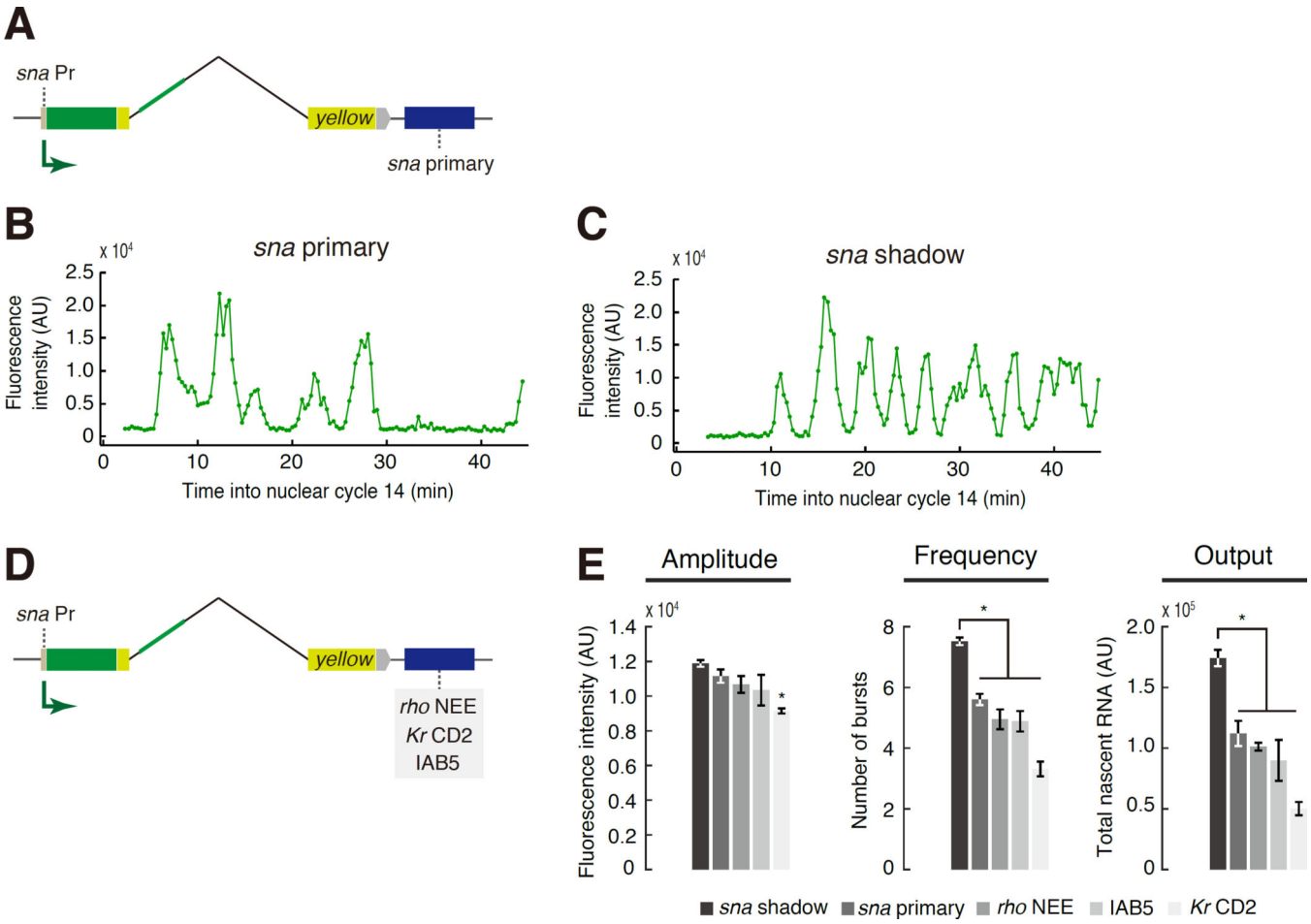

Figure 2. Bursting frequencies correlate with enhancer strength

(A) Schematic representation of *MS2-yellow* reporter gene containing the 2.8 kb *sna* primary enhancer. The enhancer is located 7.5 kb downstream of the *sna* promoter.

(B, C) A representative trace of transcription activity of *MS2-yellow* reporters with *sna* primary (B) and *sna* shadow (C) enhancers.

(D) Schematic representation of *MS2-yellow* reporter genes with *rho* NEE, *Kr* CD2, and IAB5 enhancers. In all cases, the enhancer is located 7.5 kb downstream of the *sna* promoter.

(E) Average values of amplitude, frequency, and output per nucleus. Totals of 907, 788, 450, 799, 413 nuclei from three independent embryos were analyzed for the reporter genes containing the *sna* shadow, *sna* primary, *rho* NEE, IAB5, and *Kr* CD2 enhancers, respectively. The error bars represent the standard deviation of the mean of three biological replicates. Output of *sna* shadow enhancer is the same as the plot in Figure 1E. Asterisk indicates $p < 0.01$ compared to *sna* shadow enhancer. (Note that these transgenes also contain a linked *snaPr-PP7-yellow* reporter gene in symmetric location; see Figure 5). See also Figure S2 and S3.

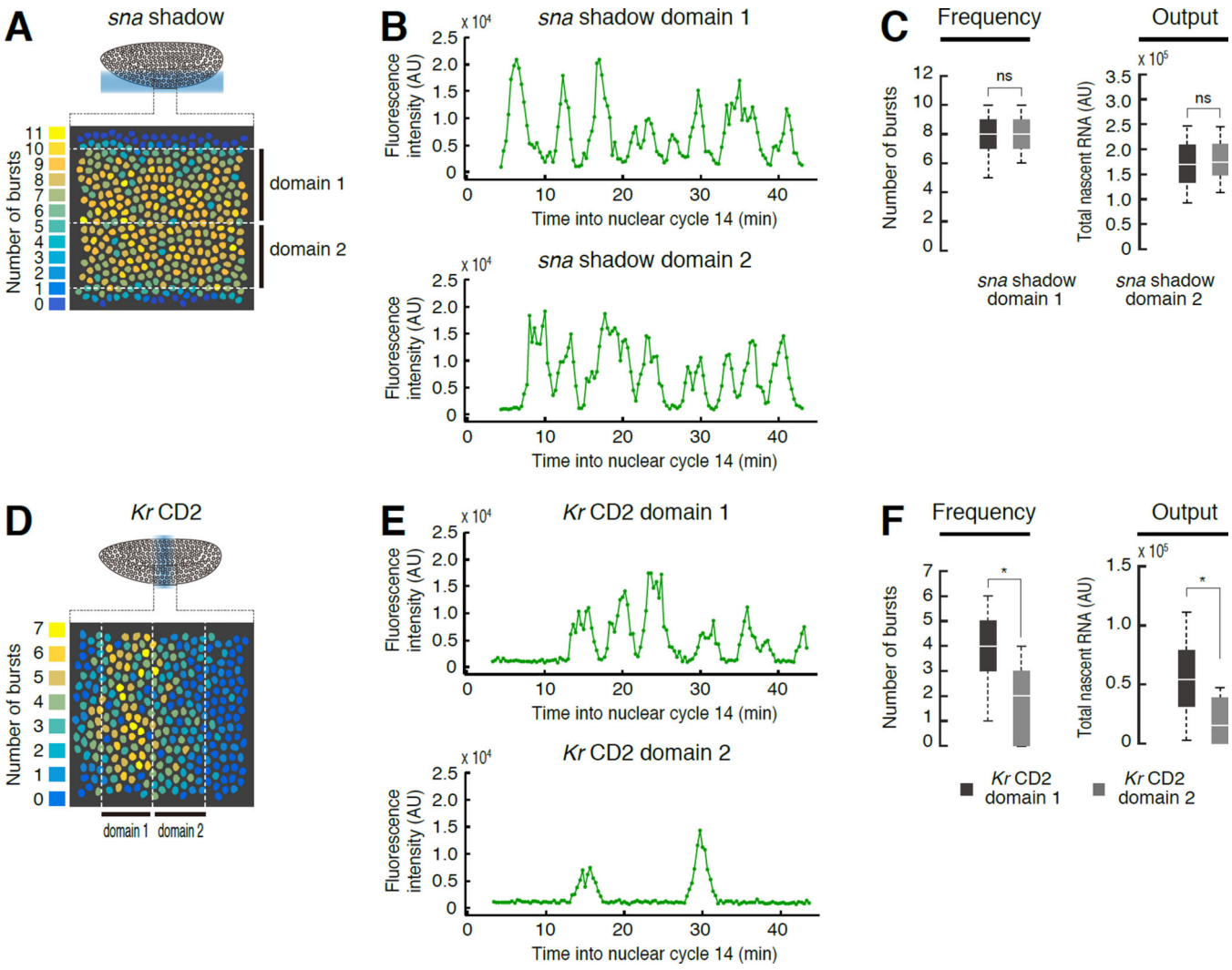

Figure 3. Differential bursting frequencies of segmentation genes

(A) Distribution of bursting frequencies in transgenic embryo expressing *snaPr-MS2-yellow* with the 3′ *sna* shadow enhancer (Figure 1B; bottom). Each nucleus is colored with respect to the total number of transcriptional bursts detected throughout nc 14. The image is oriented with anterior to the left and ventral view facing up.

(B) Representative traces of transcription activity in individual nuclei from each domain shown in (A). Each domain spans about half the total limits of the *sna* expression pattern.

(C) Boxplots showing the distribution of burst frequencies and output per nucleus in each domain shown in (A). 149 and 152 nuclei were analyzed in domains 1 and 2, respectively. The box indicates the lower (25 %) and upper (75 %) quantile and the solid line indicates the median. Whiskers extend to 10 th and 90 th percentile of each distribution.

(D) Distribution of bursting frequencies in the embryo expressing *snaPr-MS2-yellow* with the *Kr* CD2 enhancer (Figure 2D). The image is oriented with anterior to the left and dorsal up.

(E) Representative traces of transcription activity in individual nuclei from each domain shown in (D). Each domain spans about half the total limits of the *Kr* expression pattern.

(F) Boxplots showing the distribution of burst frequencies and output in each domain shown in (D). 110 and 114 nuclei were analyzed in domains 1 and 2, respectively. The box indicates the lower (25 %) and upper (75 %) quantile and the solid line indicates the median. Whiskers extend to 10 th and 90 th percentile of each distribution. Asterisk indicates $p < 0.01$. See also Figure S4 and S5.

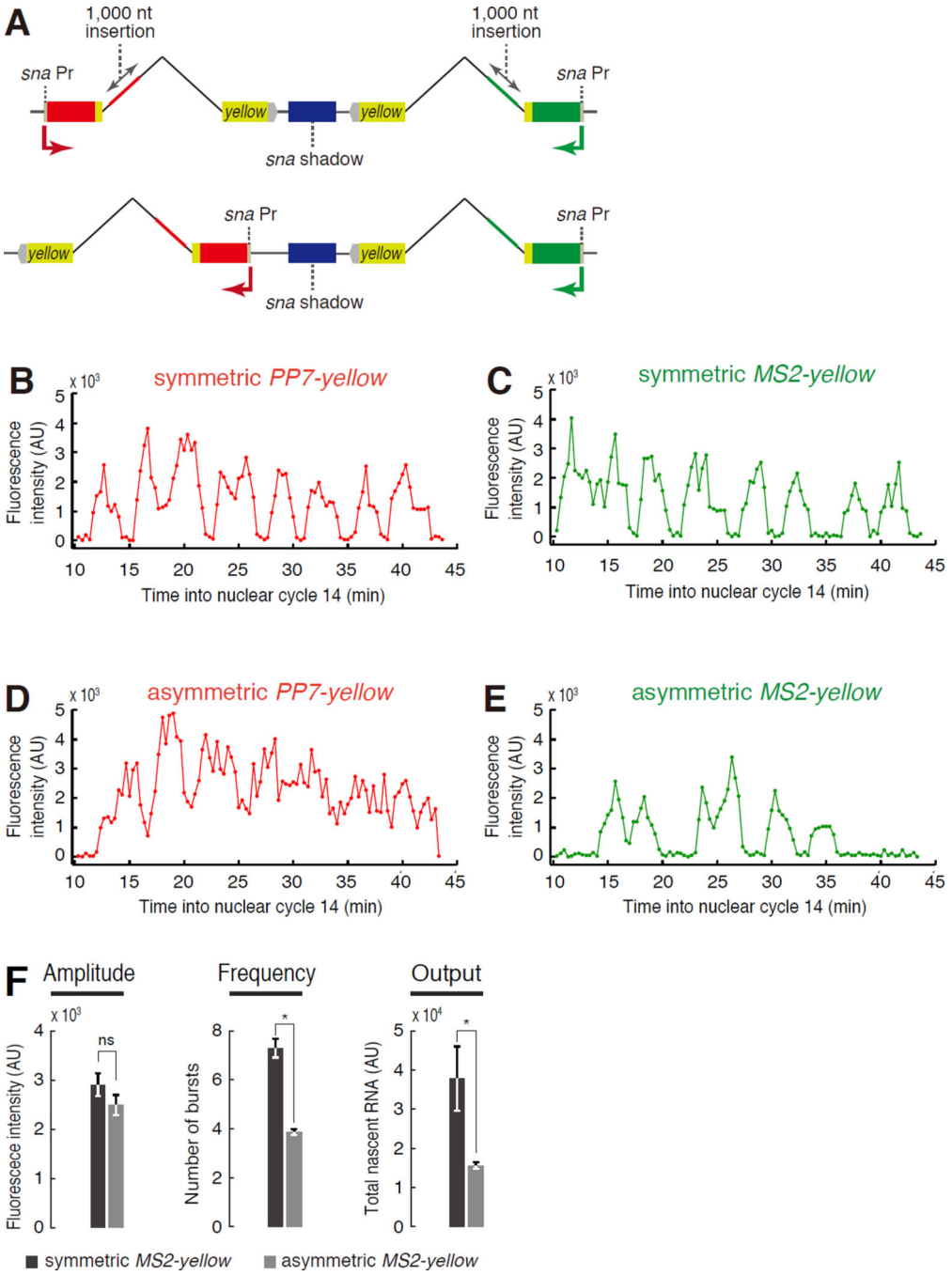

Figure 4. Promoter competition diminishes bursting frequencies

(A) Schematic representation of *snaPr-MS2-yellow* and *snaPr-PP7-yellow* reporter genes with the *sna* shadow enhancer. *snaPr-PP7-yellow* is located either 7.6 kb (symmetric; top) or 1 kb (asymmetric; bottom) from the enhancer. In both cases, the shared enhancer is located 7.5 kb from the *snaPr-MS2-yellow* reporter.

(B, C) Representative traces of transcription activity of *PP7-yellow* and *MS2-yellow* in symmetric configuration.

(D, E) Representative traces of transcription activity of *PP7-yellow* and *MS2-yellow* in asymmetric configuration (e.g., the shared enhancer is located near the *PP7-yellow* reporter). (F) Average amplitude, frequency and output per nucleus in the symmetric and the asymmetric reporter constructs. Totals of 604 and 332 nuclei from three independent embryos were analyzed for *MS2-yellow* signals in symmetric and asymmetric configurations, respectively The error bars represent the standard deviation of the mean of three biological replicates. Asterisk indicates $p < 0.01$.

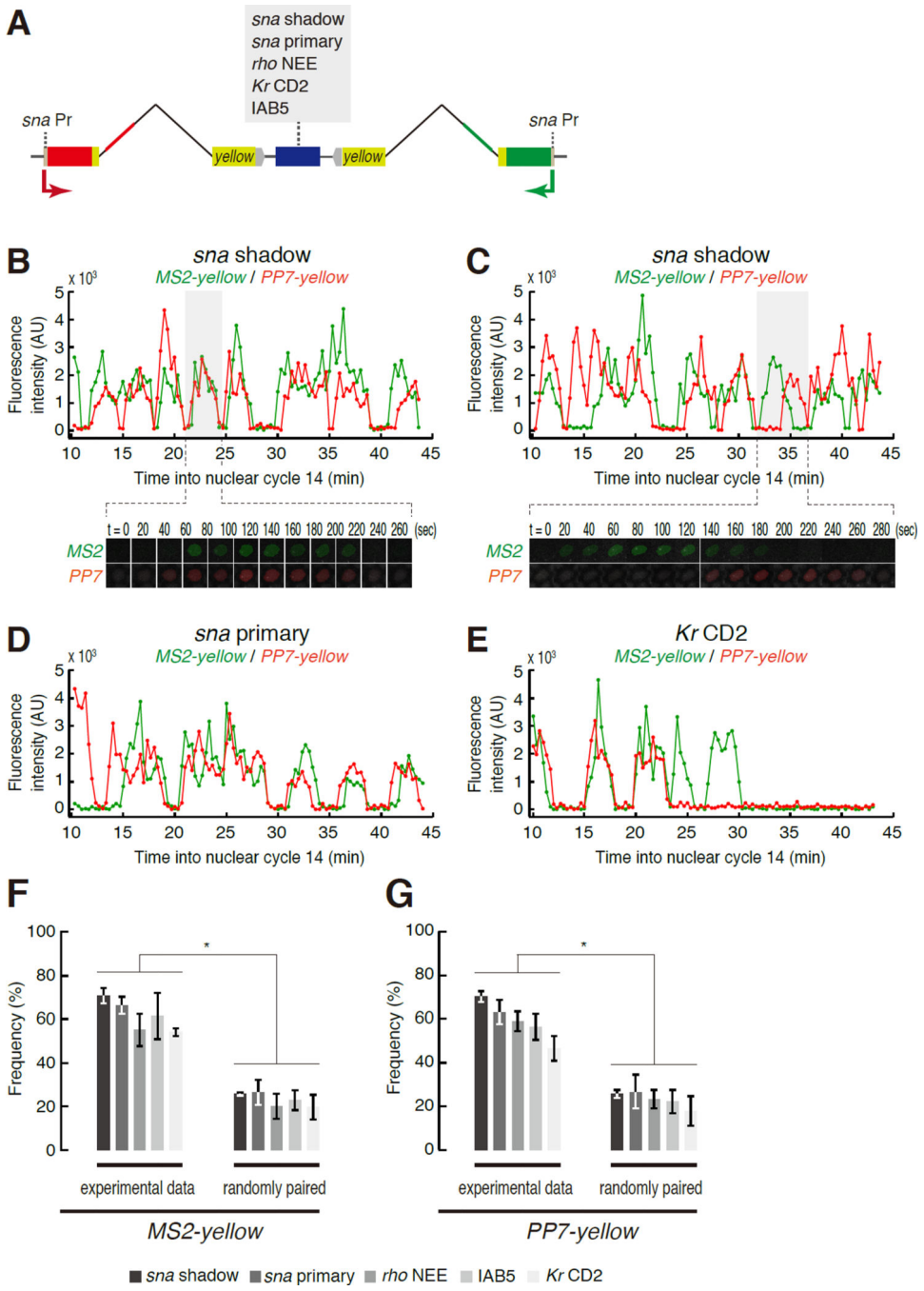

Figure 5. Coordinated transcriptional bursts by a shared enhancer

(A) Schematic representation of the symmetric *snaPr-MS2-yellow* and *snaPr-PP7-yellow* reporters with different enhancers (*sna* shadow, *sna* primary, *rho* NEE, *Kr* CD2, and IAB5). (B, C) Representative traces of transcription activity in the reporter gene with the *sna* shadow enhancer. Snapshots are taken from the nucleus that corresponds to the indicated traces. The intensity of green (*MS2-yellow*) and red (*PP7-yellow*) false-coloring is proportional to the signal strength of transcription focus at a given time.

(D, E) Representative traces of transcription activity of *MS2-yellow* and *PP7-yellow* reporters with *sna* primary (D) and *Kr* CD2 enhancers (E).

(F, G; left) Frequency of the coordinate transcriptional burst among total *MS2-yellow* (F) and *PP7-yellow* bursts (G). The error bars represent the standard deviation of the mean of three biological replicates. 613, 502, 382, 369, and 803 nuclei were analyzed for *sna* shadow, *sna* primary, IAB5, *rho* NEE, and *Kr* CD2 enhancers, respectively.

(F, G; right) Frequency of coordinate bursts among randomly paired traces. From a pool of MS2 and PP7 traces in a given embryo, traces with comparable bursting frequency were randomly paired and the number of coordinate bursts was counted. The error bars represent the standard deviation of the mean of three biological replicates. Totals of 613, 477, 310, 249 and 365 nuclei were analyzed for *sna* shadow, *sna* primary, IAB5, *rho* NEE, and *Kr* CD2 enhancers, respectively. Asterisk indicates $p < 0.01$. See also Figure S6 and S7.

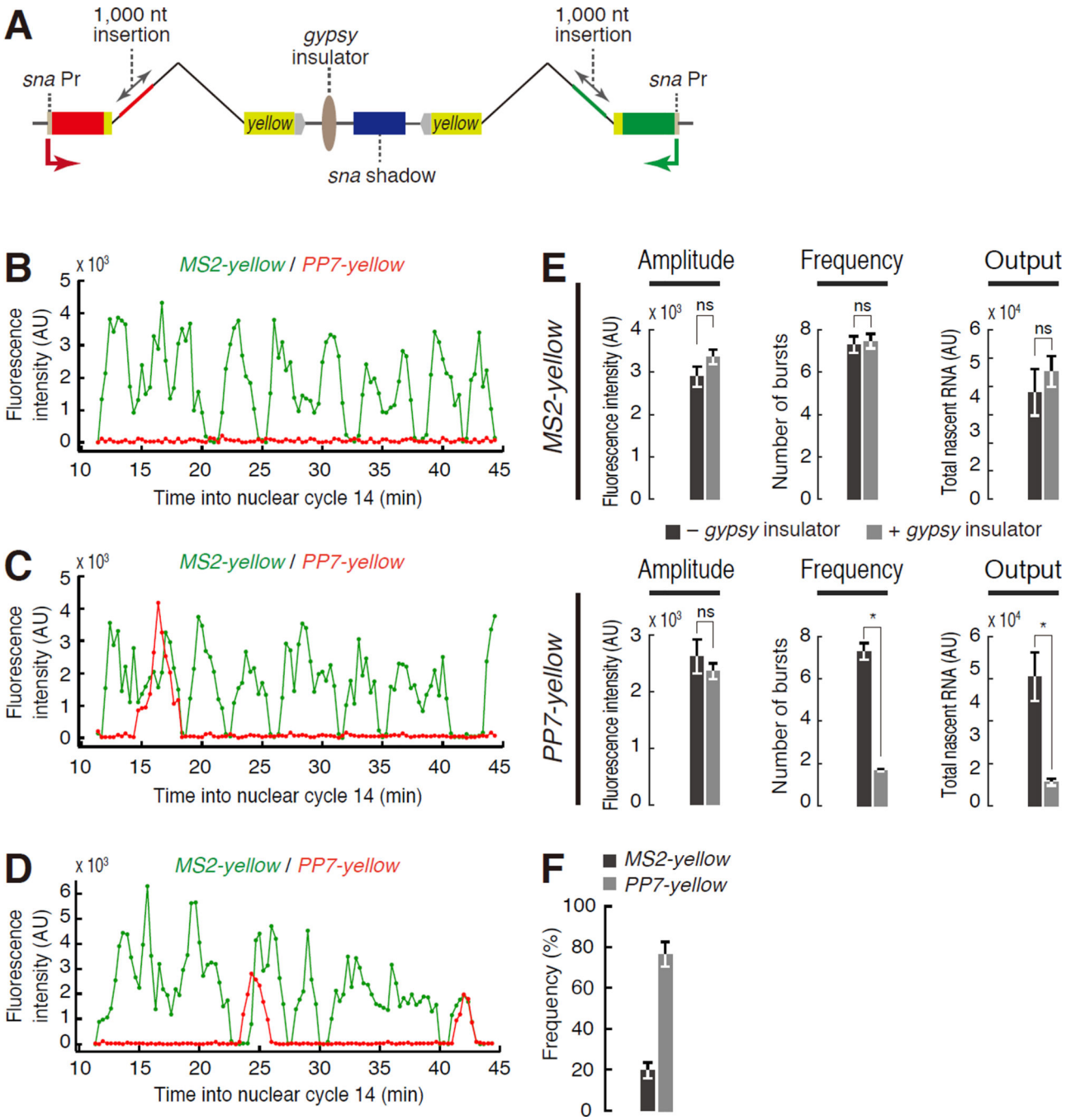

Figure 6. The *gypsy* insulator alters bursting frequencies

(A) Schematic representation of the symmetric *snaPr-MS2-yellow* and *snaPr-PP7-yellow* reporter genes with the *gypsy* insulator inserted between the *sna* shadow enhancer and *snaPr-PP7-yellow*.

(B–D) Representative traces of transcription activity of *MS2-yellow* and *PP7-yellow*. (E) Average amplitude, frequency and output per nucleus in the reporter constructs with or without the insulator. Total of 604 and 579 nuclei from three independent embryos were analyzed for the reporters without and with the insulator, respectively. The plot shown in

Figure 4F (symmetric *MS2-yellow*) was used for the reporter without the insulator. The error bars represent the standard deviation of the mean of three biological replicates. Asterisk indicates $p < 0.01$.

(F) Frequency of coordinate transcriptional bursts among total *MS2-yellow* and *PP7-yellow* bursts. The error bars represent the standard deviation of the mean of three biological replicates and 579 nuclei were analyzed.

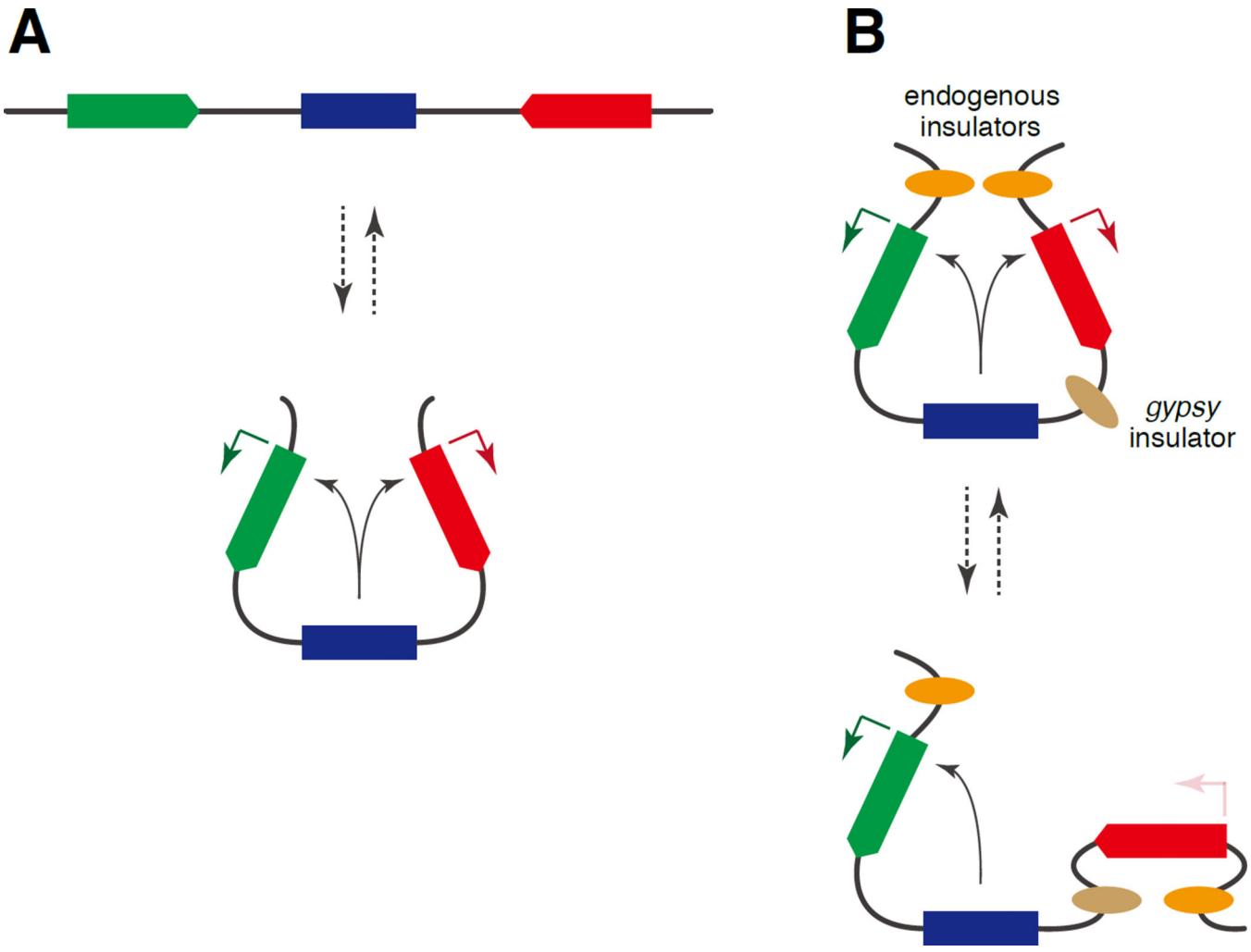

Figure 7. A model for dynamic transitions in chromosome topology

(A) A model for the coordinated activation of two-linked reporter genes by a shared enhancer. A higher order chromosomal loop domain positions the shared enhancer near both target promoters. (B) We propose that the *gypsy* insulator blocks enhancer-promoter interactions by forming a chromosomal loop domain by pairing with a nearby endogenous insulator (bottom). The occasional coordinated bursts that are observed can be explained by dynamic conformational changes in chromosomal loop domains.